The fundamental metallicity relation from $z \sim 0$ to $z \sim 0.7$: Selection or Evolution?

Francesco Pistis[1], Agnieszka Pollo[1·2], Marco Scodeggio[3], Miguel Figueira[1], Anna Durkalec[1], Katarzyna Małek[1·4], Angela Iovino[5], Daniela Vergani[6] and Samir Salim[7]

1. National Centre for Nuclear Research, ul. Pasteura 7, 02-093 Warsaw, Poland
2. Astronomical Observatory of the Jagiellonian University, Orla 171, 30-001 Cracow, Poland
3. INAF - Istituto di Astrofisica Spaziale e Fisica Cosmica Milano, via Bassini 15, 20133, Milano, Italy
4. Aix Marseille Univ. CNRS, CNES, LAM, Marseille, France
5. INAF - Osservatorio Astronomico di Brera, Via Brera 28, 20122 Milano, via E. Bianchi 46, 23807 Merate, Italy
6. INAF - Osservatorio di Astrofisica e Scienza dello Spazio di Bologna, Via Piero Gobetti 93/3, I-40129 Bologna, Italy
7. Department of Astronomy, Indiana University, Bloomington, Indiana 47405, USA

Galaxy metallicity, as a result of the integrated star formation history and evolution of the interstellar medium, is an important property describing galaxy evolution. Its relation with galaxy stellar mass and star formation rate (SFR), known as the fundamental metallicity relation (FMR), has been widely studied, especially in the local Universe. However, when it comes to the evolution of the FMR, most of the studies are based on very different samples, with different data selections at different redshift ranges. We check how different selection biases affect the FMR projections. This will allow us to separate the real physical evolution from the false evolution introduced by these biases. We find significant differences between FMR projections occurring when different ways of data selection, simulating the selection of higher redshift samples, are applied to the SDSS data at $z \sim 0$. Then, we compare the results with the findings from the VIPERS sample at $z \sim 0.7$. We conclude that both FMR and its projections at $z \sim 0.7$ and $z \sim 0$ are in good agreement. When the data selection effects are carefully applied the differences between samples are reduced, especially at high stellar mass, but these biases are not able to reproduce the flattening at low stellar mass showed by the sample at $z \sim 0.7$.

1 Introduction

Most chemical elements are formed inside stars during their evolution. The metal content is a measure of the integrated star formation history (SFH) and it depends both on inflow of metal-poor and outflow of metal-rich gas. Since different elements are formed on different timescales by different star populations, their relative abundances constrain the SFH. A galaxy is a system in communication with the gas in the intergalactic medium (IGM). The metal-poor gas inflows into the galaxy where it ignites the formation of new stars and it is processed by their evolution. The stellar population enriches the interstellar medium (ISM) by, e.g., supernovae and stellar winds. The metal-enriched gas can eventually leave the galaxy by galactic winds (Maiolino & Mannucci, 2019). From this point of view, the main galaxy properties, such as stellar mass (M_*), star formation rate (SFR), and gas-phase metallicity (Z), are strongly connected.

The Fundamental Metallicity Relation (FMR) was first introduced based on the data from the Sloan Digital Sky Survey (SDSS) at redshift $z \sim 0$ and with very

good statistics ($\sim 150\,000$ star forming galaxies, Mannucci et al., 2010). The FMR is a surface where each galaxy is placed in a 3D space described by stellar mass, SFR, and metallicity. Adding the SFR dependence to the Mass Metallicity Relation (MZR) reduced the dispersion of the relation. The stellar mass dependence is in agreement with the downsizing model and models taking into account the outflow. At the same time, the SFR dependence is also in agreement with models taking into account the dilution by inflow. Mannucci et al. (2010) compared also the FMR for different values of redshift and they do not find any evolution up to $z \sim 2.5$.

The studies of evolution of these relations are mainly restricted to the MZR. Savaglio et al. (2005) studied ~ 60 galaxies from the Gemini Deep Deep Survey (GDSS) and Canada-France Redshift Survey (CFRS) with redshifts $0.4 \leq z \leq 1.0$. They found a shift of the MZR with redshift. This observation is in agreement with a closed-box galaxy model.

From the theoretical point of view, Lian et al. (2018a,b) described the MZR evolution with models based on time-dependent outflow or the Initial Mass Function (IMF). They found a two-phase evolution: the MZR evolves shifting parallel to itself without changing slope up to $z \sim 1.5$, and then, it starts to flatten until today.

2 Data

2.1 VIPERS sample

We use a sample from the VIMOS Public Extragalactic Redshift Survey (VIPERS, Guzzo & VIPERS Team, 2013; Garilli et al., 2014; Scodeggio et al., 2018). This is a spectroscopic sample of $\sim 90\,000$ galaxies with a magnitude limit $i_{\rm AB} < 22.5$ and an observed sky area of 25.5 deg^2. We cross-match this catalog with the one used in Turner et al. (2021) where galaxy properties were estimated by spectral energy distribution (SED) fitting with the Code Investigating GALaxy Emission (CIGALE, Burgarella et al., 2005; Noll et al., 2009; Boquien et al., 2019). This catalog is built from the photometric catalog prepared by Moutard et al. (2016a,b). It contains physical properties of galaxies (stellar mass, SFR, and absolute magnitudes).

To guarantee high accuracy, we select galaxies with secure redshift ($> 90\%$ confidence level; Scodeggio et al., 2018). We limit the redshift sample to $z_{\rm max} \sim 0.9$ to be sure to have measurements of all the emission lines we need to estimate the metallicity. The fluxes are corrected for attenuation, for both host galaxy and Milky Way extinctions, following Cardelli et al. (1989) assuming $R_V = 3.1$. The extinction due to the host galaxy is estimated with the attenuation in the V-band ($A_{\rm V}$) provided by the fit of the SED via the code Hyperz (Bolzonella et al., 2000, 2010). The extinction due to the Milky Way is estimated with the color excess $\mathrm{E\,(B-V)}$ derived from sky maps (Schlegel et al., 1998). In addition, the Hβ line is corrected for stellar absorption via the Hopkins et al. (2003) formula:

$$S = \frac{EW + EW_{\rm C}}{EW} F\,, \tag{1}$$

where S is the stellar absorption corrected line flux, EW is the equivalent width of the line, $EW_{\rm C}$ is the correction for stellar absorption, and F is the line flux already corrected for attenuation via Cardelli et al. (1989). We adopted the commonly used in the literature value of $EW_{\rm C} = 2$ Å (Miller & Owen, 2002; Goto et al., 2003).

The redshift range and the wavelength coverage of VIPERS do not allow for the detection of the [N II] λ6584 and Hα lines. For this reason, to select only star-forming galaxies and separate them from the Active Galactic Nuclei (AGNs) we used the diagram proposed by Lamareille (2010) instead of the usual Baldwin, Phillips & Terlevich diagrams (BPT, Baldwin et al., 1981). The total number of star-forming galaxies selected in this way in VIPERS is 4772.

2.2 SDSS sample

As the low-z comparison sample we choose SDSS. This sample was already used in many studies of MZR and FMR (e.g., Tremonti et al., 2004; Mannucci et al., 2010; Salim et al., 2014; Curti et al., 2020). SDSS observed spectroscopically 9380 deg^2 of the sky which makes it the most extended spectroscopic survey at low redshift. This comparison sample is built by cross-matching two different samples.

Flux sample: the MPA/JHU catalogue[1] based on the SDSS DR7[2] (Abazajian et al., 2009) composed of 927 552 galaxies with spectroscopic redshift and line fluxes (Kauffmann et al., 2003; Brinchmann et al., 2004; Tremonti et al., 2004);

Physical properties sample: the A2.1 version of the GALEX-SDSS-WISE Legacy Catalog[3] (GSWLC-2, Salim et al., 2016, 2018) with 640 659 galaxies, based on SDSS DR10 (Ahn et al., 2014) with GALEX and WISE at $z < 0.3$. This catalog contains physical properties (stellar mass, SFR, and magnitudes) obtained through SED fitting with CIGALE.

In the end, this cross-matched sample is composed of 601 082 galaxies. For this sample, we followed the data selection described by Curti et al. (2020): we select galaxies with a signal to noise ratio (S/N) equal to at least 15 for Hα, and equal to at least 3 for Hβ. Then, we corrected all emission lines for attenuation from the measured Balmer decrement, assuming the case of B recombination (Hα/Hβ = 2.87) and adopting the Cardelli et al. (1989) law assuming $R_V = 3.1$. Finally, we removed all galaxies with high extinction, i.e. with values of E (B − V) higher than 0.8. Star-forming galaxies are selected in the same way as in the VIPERS sample. The final sample contains 156 018 galaxies.

3 Possible biases

Since the FMR depends on three galactic properties, we need to compare different samples with the most consistent measurements. The stellar mass is estimated via SED fitting using CIGALE for both samples. The SFR are estimated from the [O II] luminosity ($L_{[O\,II]}$, Kennicutt, 1998). The metallicity is estimated via the ratio

$$R_{23} = \frac{[\mathrm{O\,II}]\,\lambda 3727 + [\mathrm{O\,III}]\,\lambda\lambda 4959, 5007}{\mathrm{H}\beta}\,, \tag{2}$$

using the calibration described by Tremonti et al. (2004).

Then we checked if data selection (signal-to-noise ratio, S/N, and quality of the spectra) or physical selection (range in B − B* and fraction of blue galaxies) affect

[1] https://wwwmpa.mpa-garching.mpg.de/SDSS/DR7/
[2] http://classic.sdss.org/dr7/
[3] https://salims.pages.iu.edu/gswlc/

the FMR and its projections and if these selections can possibly mimic an evolution. The main results can be summarized as follows.

S/N: we cut the SDSS sample on S/N equal to that of the VIPERS sample and with different best-percentages. This selection has the effect to remove metal-rich galaxies at high stellar mass and low SFR.

Spectrum quality: this selection is based on the condition of S/N on flux and equivalent width of the emission lines — i.e., it is more sophisticated than the simple S/N selection. We also analyzed the effects for each emission line. The overall effects are similar to the simple S/N selection but the strongest bias is introduced by the requirement of high S/N of [O III] λ4959.

Range in $B - B^*$: selection on the absolute blue magnitude of the galaxies normalized with respect to B^*, which is the characteristic Schechter magnitude at which the luminosity function changes behavior at a given redshift. In this way we study galaxies of comparable luminosities with respect to the luminosity function evolution. This selection has the only effect to remove metal-rich galaxies at high SFR and to shift a little the main sequence towards lower stellar mass and SFR.

Fraction of blue galaxies: this selection accounts for two effects. I) blue galaxies are more difficult to observe at high redshift due to their lower mass and are not observed because of the limited magnitude of the survey; II) this type of galaxies can be over-selected at high redshift because strong emission lines make them easier to identify — in particular, the VIPERS i-band selection translates to a B-band selection at $z \sim 0.7$ and for galaxies with bright emission lines it is easier to estimate their metallicity. In our case, the only affected projection is the main sequence with a stronger shift as compared to the selection on luminosity.

4 Evolution of the fundamental metallicity relation?

We then proceeded to apply simultaneously all biases to the SDSS sample and compare it with the VIPERS sample. Figure 1 shows the effects on different FMR projections. Taking into account the considered biases does not have significant effects to change the FMR projections. The biases considered are not able to reproduce the characteristics of the VIPERS sample such as the flattening at low stellar mass in the MZR.

Figure 2 shows the metallicity difference $\Delta \log(\mathrm{O/H})$ in each stellar mass-SFR bin for both cases with and without biases considered. The smallest difference is towards the top-left corner of the main sequence where VIPERS sample shows a flattening. Taking into account the biases reduces the average difference from $\sim 0.5 \langle s_{\mathrm{VIPERS}} \rangle = 0.08$ dex to $\sim 0.4 \langle s_{\mathrm{VIPERS}} \rangle = 0.06$ dex, mainly at large stellar mass.

5 Conclusions

The VIPERS sample is in a good agreement with the local sample with standard data selection, $\sim 0.5 \langle s_{\mathrm{VIPERS}} \rangle$ in the FMR. The biases taken into account are able to reduce the metallicity difference between these samples to $\sim 0.4 \langle s_{\mathrm{VIPERS}} \rangle$, but they are not able to reproduce the characteristics of the VIPERS sample such as the flattening at low stellar mass in the MZR.

Data selection such as S/N cutoffs and flag quality of the spectra affects the

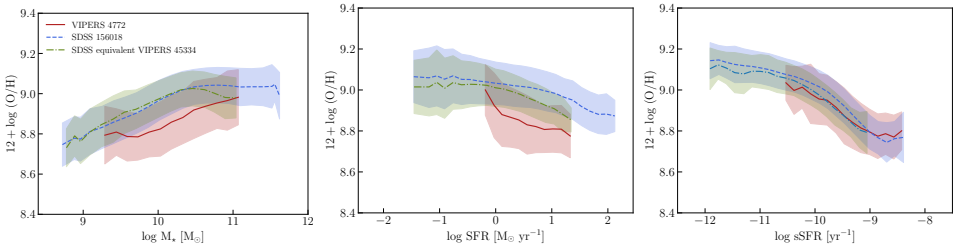

Fig. 1: Three projections of the FMR: MZR (*left*), metallicity vs SFR (*mid right*), metallicity vs sSFR (*right*) for VIPERS (red), SDSS (blue), and SDSS equivalent to VIPERS (green) samples.

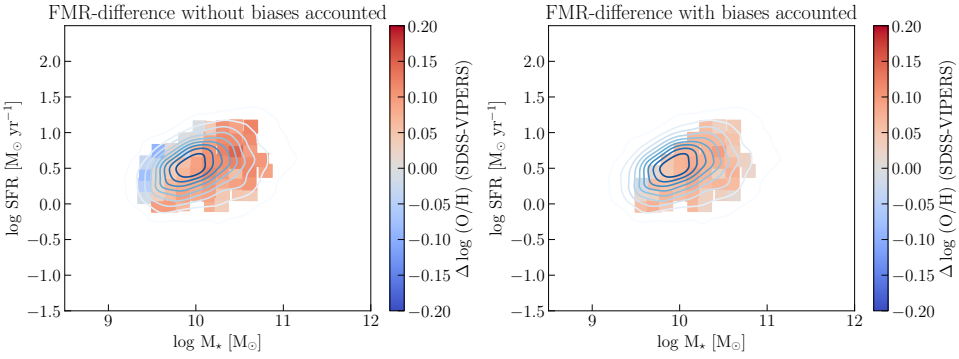

Fig. 2: Difference between FMRs of SDSS without (*left*) and with (*right*) biases accounted for and VIPERS projected on the main sequence of VIPERS sample (KDE contour plot).

MZR and the plane metallicity vs SFR leading to nonphysical relations, e.g., hiding the anti-correlation between the galactic properties in the plane metallicity vs SFR and fall-off of the MZR at large stellar mass, which can be mistaken as evidence of evolution. These kinds of selections can introduce biases if applied to the oxygen lines, especially if applied to [O III] λ4959. More details can be found in Pistis et al. (2022).

Among all the FMR projections, the metallicity vs sSFR (specific SFR defined as the ration between SFR and M_*) is the least sensitive to biases. For this reason a non-parametric framework (Salim et al., 2014, 2015) can be a better way than the study of the FMR projections, since an evolution of the projections is not reflected into the FMR itself. This approach will be further explored in Pistis et al. (in prep.).

Acknowledgements. This research was supported by the Polish National Science Centre grant No. UMO-2018/30/M/ST9/00757. This paper uses data from the VIMOS Public Extragalactic Redshift Survey (VIPERS[4]). VIPERS has been performed using the ESO Very Large Telescope, under the "Large Programme" 182.A-0886. We thank B. Garilli for the line measurements for the VIPERS sample. This research made use of Astropy,[5] a

[4] `http://vipers.inaf.it`
[5] `http://www.astropy.org`

community-developed core Python package for Astronomy (Astropy Collaboration et al., 2013, 2018).

References

Abazajian, K. N., et al., *ApJS* **182**, 2, 543 (2009)

Ahn, C. P., et al., *ApJS* **211**, 2, 17 (2014)

Astropy Collaboration, et al., *A&A* **558**, A33 (2013)

Astropy Collaboration, et al., *AJ* **156**, 3, 123 (2018)

Baldwin, J. A., Phillips, M. M., Terlevich, R., *PASP* **93**, 5 (1981)

Bolzonella, M., Miralles, J. M., Pellò, R., *A&A* **363**, 476 (2000)

Bolzonella, M., et al., *A&A* **524**, A76 (2010)

Boquien, M., et al., *A&A* **622**, A103 (2019)

Brinchmann, J., et al., *MNRAS* **351**, 4, 1151 (2004)

Burgarella, D., Buat, V., Iglesias-Páramo, J., *MNRAS* **360**, 4, 1413 (2005)

Cardelli, J. A., Clayton, G. C., Mathis, J. S., *ApJ* **345**, 245 (1989)

Curti, M., Mannucci, F., Cresci, G., Maiolino, R., *MNRAS* **491**, 1, 944 (2020)

Garilli, B., et al., *A&A* **562**, A23 (2014)

Goto, T., et al., *PASJ* **55**, 771 (2003)

Guzzo, L., VIPERS Team, *The Messenger* **151**, 41 (2013)

Hopkins, A. M., et al., *ApJ* **599**, 2, 971 (2003)

Kauffmann, G., et al., *MNRAS* **341**, 1, 33 (2003)

Kennicutt, J., Robert C., *ARA&A* **36**, 189 (1998)

Lamareille, F., *A&A* **509**, A53 (2010)

Lian, J., Thomas, D., Maraston, C., *MNRAS* **481**, 3, 4000 (2018a)

Lian, J., et al., *MNRAS* **474**, 1, 1143 (2018b)

Maiolino, R., Mannucci, F., *A&A Rev.* **27**, 1, 3 (2019)

Mannucci, F., et al., *MNRAS* **408**, 4, 2115 (2010)

Miller, N. A., Owen, F. N., *AJ* **124**, 5, 2453 (2002)

Moutard, T., et al., *A&A* **590**, A102 (2016a)

Moutard, T., et al., *A&A* **590**, A103 (2016b)

Noll, S., et al., *A&A* **507**, 3, 1793 (2009)

Pistis, F., et al., *A&A* **663**, A162 (2022)

Salim, S., Boquien, M., Lee, J. C., *ApJ* **859**, 1, 11 (2018)

Salim, S., Lee, J. C., Davè, R., Dickinson, M., *ApJ* **808**, 1, 25 (2015)

Salim, S., et al., *ApJ* **797**, 2, 126 (2014)

Salim, S., et al., *ApJS* **227**, 1, 2 (2016)

Savaglio, S., et al., *ApJ* **635**, 1, 260 (2005)

Schlegel, D. J., Finkbeiner, D. P., Davis, M., *ApJ* **500**, 2, 525 (1998)

Scodeggio, M., et al., *A&A* **609**, A84 (2018)

Tremonti, C. A., et al., *ApJ* **613**, 2, 898 (2004)

Turner, S., et al., *MNRAS* **503**, 2, 3010 (2021)